Polarization of Valence Band Holes in the (Ga,Mn)As Diluted Magnetic Semiconductor

V. F. Sapega,* M. Moreno,† M. Ramsteiner, L. Däweritz, and K. H. Ploog
Paul-Drude-Institut für Festkörperelektronik, Hausvogteiplatz 5–7, D-10117 Berlin, Germany
(Received 19 October 2004; published 4 April 2005)

We report on direct measurements of the impurity band hole polarization in the diluted magnetic semiconductor (Ga,Mn)As. The polarization of impurity band holes in a magnetic field is strongly enhanced by antiferromagnetic exchange interaction with Mn ions. The temperature dependence of the hole polarization shows a strong increase of this polarization below the Curie temperature. We show that the ground state of the impurity band is formed by uniaxial stress split $F = \pm 1$ states of antiferromagnetically coupled Mn ions ($S = 5/2$) and valence band holes ($J = 3/2$). The gap between the Mn acceptor related impurity band and the valence band is directly measured in a wide range of Mn content.

DOI: 10.1103/PhysRevLett.94.137401 PACS numbers: 78.30.Fs, 75.50.Pp, 76.30.Pk

The discovery of ferromagnetism in the (Ga,Mn)As diluted magnetic semiconductor (DMS) [1] opens new prospects for realizing semiconducting spintronics devices [2,3]. The effect of magnetic Mn ions on the transport of free carriers as well as the reverse effect of spin polarized photogenerated carriers on ferromagnetically coupled Mn spins have recently been observed in several experiments [1,4–6]. These experiments clearly indicate the mutual influence of magnetic ions and free carriers. However, in spite of a great deal of recent theoretical activities [7–14], there is no complete understanding of the origin of ferromagnetism in this material system. In view of the ongoing experiments on electrical spin injection from (Ga,Mn)As, an important question arises about the degree of hole spin polarization as a function of sample magnetization. Furthermore, the correlation between hole polarization and sample magnetization as well as hole state (mobile or localized) and its Fermi energy is important to distinguish between different theoretical approaches.

In this Letter, we present a direct study of the valence band hole polarization in a wide range of temperatures in (Ga,Mn)As DMSs by means of hot-electron photoluminescence (HPL) [15,16]. The HPL spectrum and its circular polarization in a magnetic field provide information on the acceptor binding energy and the polarization of holes bound to single Mn acceptors [17] or in the acceptor impurity band. Here, our study of the HPL spectra demonstrates that in a wide range of Mn content the valence band holes predominantly occupy the Mn acceptor impurity band even for the highest Mn concentration samples and can therefore not play the role of a Fermi sea in the Rudermann-Kittel-Kasuya-Yosida- (RKKY-)like exchange interaction. Furthermore, the HPL polarization study indicates that a random strong stress existing in (Ga,Mn)As DMSs removes the threefold degeneracy of the ground $F = 1$ (antiferromagnetically coupled $3d^5$ electrons of Mn ions and valence band holes) state on two $F = 0$ and $F = \pm 1$ sublevels, the latter being the ground state. The temperature activated transition into the spin unpolarized state $F = 0$ can thus determine the Curie temperature of this system.

The 500 nm thick (Ga,Mn)As films for this study were grown at 250 °C by molecular beam epitaxy on semi-insulating GaAs(001) substrates covered with 100 nm GaAs buffer layers. Three of the samples have a Mn content of $x = 0.01$ ($B1$), $x = 0.04$ ($B2$), and $x = 0.043$ ($B3$). In addition, a Mn-doped ($\sim 3 \times 10^{17}$ cm^{-3}) 1000 nm thick GaAs film grown at 540 °C was used as reference sample A. Superconducting-quantum-interference-device (SQUID) measurements were carried out in the temperature range 5–400 K to investigate the macroscopic magnetic properties of the samples and to confirm the absence of MnAs nanoclusters. The SQUID measurements showed ferromagnetic (FM) behavior of samples $B2$ and $B3$ with Curie temperatures $T_C = 35$ and 55 K, respectively, while sample $B1$ was paramagnetic (PM). For HPL excitation, we used the lines of a He-Ne and a Kr-ion laser. The laser power densities focused on the sample ranged from 5 to 50 W cm^{-2}. The experiments in the temperature range 4–200 K were carried out in a continuous He-flow cryostat using magnetic fields up to 12 T in the backscattering Faraday geometry.

Sample A shows near-band-gap photoluminescence (PL) due to the recombination of photoexcited free electrons with holes bound to neutral Mn acceptors ($e - A^0$); the PL band is centered at 1.411 eV [18]. In the (Ga,Mn)As, DMS samples of group B, with Mn content $0.01 < x \leq 0.05$, we did not detect any near-band-gap PL. The common feature of both sample types is a weak HPL. Figure 1 shows the HPL spectra obtained from the samples A, $B1$, and $B3$ under He-Ne laser excitation at a temperature of $T = 5$ K (similar spectra were observed under Kr-ion laser excitation with $E_{ex} = 1.833$ eV). Under cw excitation laser photons excite electrons from the heavy-hole subband (we will discuss only this channel of excitation because of the larger density of states in this subband as compared to the light-hole subband) into the conduction band [see inset (b) in Fig. 1]. The electrons subsequently relax toward the Γ band minimum by emission of LO phonons in moderately doped samples or by electron-hole scattering in heavily doped ones. The radiative recombination of these nonequilibrium electrons with

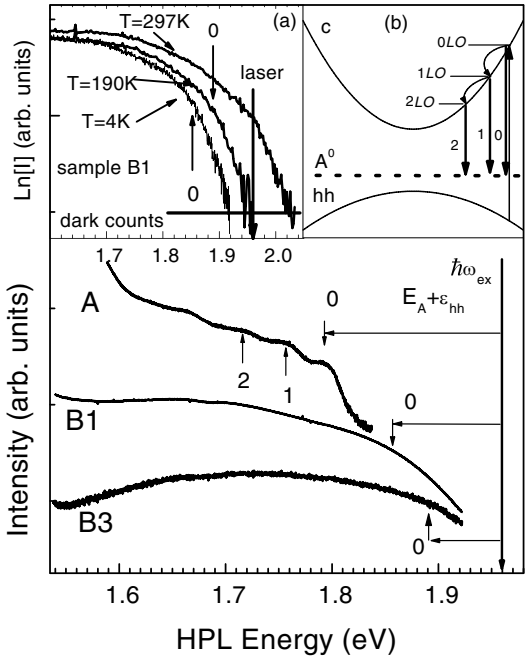

FIG. 1. HPL spectra of (Ga,Mn)As for samples of type A, $B1$, and $B3$ excited with $\hbar\omega_{ex} = 1.96$ eV at $T = 5$ K. The arrows labeled as 0 indicate the energy for the recombination of electrons from the point of generation. Inset (a) shows HPL spectra of sample $B1$ for three different temperatures. Inset (b) explains the origin of HPL.

acceptor-bound holes (A^0) then leads to the HPL spectrum, which spreads from the point of generation (marked as "0" on the high-energy side of the spectra) to the bottom of the conduction band [15–17].

The starting point of the HPL spectrum 0 is determined for a monoenergetic acceptor (spectrum of sample A in Fig. 1) by the simple expression [see inset (b) in Fig. 1] $\hbar\omega_0 = \hbar\omega_{ex} - E_A - \varepsilon_{hh}$, where $\hbar\omega_{ex}$, is the excitation laser energy, $E_A = 113$ eV [18] is the acceptor binding energy, and ε_{hh} is the kinetic energy of heavy holes determined by the dispersion of the hh band (for fixed excitation with the He-Ne laser $\hbar\omega_{ex} = 1.959$ eV, the value $\varepsilon_{hh} = 0.048$ eV is also fixed). The broadening of the acceptor state with increasing Mn content and the following impurity band formation leads to the shift of the HPL starting point 0 toward the excitation energy (spectra of samples $B1$ and $B3$). The effective energy gap between the impurity band and the valence band can thus be directly measured. This gap is equal to the Mn single acceptor binding energy in the doping regime $E_A = 0.113$ eV and tends to $\Delta = 0.021$ eV in the sample with the highest Mn content $x = 0.043$. The temperature increase leads to the thermal excitation of the acceptor or impurity band bound holes into the valence band. The appearance of free holes in the valence band can be detected as additional contribution in HPL intensity [see inset (a) in Fig. 1] near excitation laser line (due to direct e-hh optical transition) [19]. The contribution of free holes into HPL intensity becomes noticeable only at temperature $T \geq 100$–200 K (depending on Mn content), thus supporting our assumption on localized character of holes in DMS at low temperatures.

The characteristic feature of HPL in GaAs is its linear polarization related to the momentum alignment of electrons due to absorption of linearly polarized light in direct interband optical transitions (see, e.g., Ref. [15]). The linear polarization of all A and B samples measured in the starting point 0 under linearly polarized excitation $\rho_l = 0.22$–0.26 is close to its theoretical limit ($\rho_l = 0.25$) [19]. Violation of the momentum conservation law in disordered DMSs thus would lead to strong suppression of HPL linear polarization. The analysis of HPL spectra (dependence on excitation energy, temperature, and its linear polarization) made above rules out alternative mechanisms of PL recombination channels such as band renormalization and disorder induced indirect transitions. This means that in a wide range of Mn content the valence band hole is either bound to the Mn acceptor or confined in the impurity band and thus far from degeneracy as assumed in the RKKY based theories [10].

Figure 2(a) shows the magnetic field dependences of circular polarization [$\rho_c = (I^+ - I^-)/(I^+ + I^-)$, where I^+ and I^- are the HPL intensities measured in σ^+ and σ^- polarization, respectively] measured in the HPL starting point for the samples A, $B1$, and $B3$. Note that the polarization curves do not depend on energy in the entire HPL spectral range. The magnetic field induced circular polarization of the HPL is exclusively related to the magnetization of the impurity holes [17]. The solid triangles in this figure represent the magnetization curve measured on

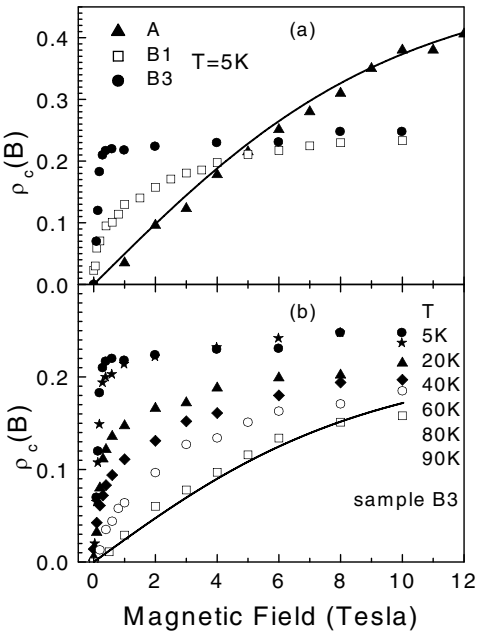

FIG. 2. Magnetic field dependences of the HPL circular polarization: (a) measured at $T = 5$ K in samples A (solid triangles), $B1$ (solid squares), and $B3$ (solid circles) as well as (b) measured at different temperature in sample $B3$. The solid lines are fits according to Ref. [20] in (a) and by using Eqs. (1) and (2) in (b).

sample A and reproduce the result of Ref. [17]. This dependence can be well fitted (solid line) by the model, assuming that holes bound to Mn acceptors antiferromagnetically coupled with $3d^5$ electrons of the inner Mn shell [17,20]. The exchange energy, the stress induced splitting of the ground state, and the acceptor g factor were measured in Ref. [21] and amount to $\Delta = 2.2$ meV, $\delta \leq 1$ meV, and $g_A = 2.74$, respectively. For these parameters ($\Delta > \delta$) the theory developed in Ref. [20] predicts a saturation of the polarization at $\rho_c = 0.504$. One can see that the transition from the doping regime (sample A) to DMSs (samples $B1$-PM and $B3$-FM) is accompanied by a decrease of the saturation polarization and a decrease of the saturating magnetic field. The decrease of the polarization in a saturating field can be understood by a model assuming that the Mn acceptors states undergo a strong stress (or electric-field) induced splitting, i.e., $|\delta| \gg kT, g_A\mu_B B$. The local stress splits the ground state of the acceptors ($F = 1$) in two sublevels with $F = \pm 1$ and $F = 0$ projections on the stress direction. In this case, the magnetic field dependence of the circular polarization reads as [17,20]

$$\rho_c(B) = \frac{18}{35}\int_0^1 y \tanh\left(\frac{y g_A \mu_B B_{\text{eff}}(B)}{kT}\right) dy, \qquad (1)$$

where $y = \cos(\vartheta)$, and ϑ is the angle between the magnetic field and stress directions. Expression (1) assumes averaging over random orientations (spherical or cubic) of stress, and in a saturating magnetic field it gives the polarization $\rho_c(\infty) = 0.257$ and $\rho_c(\infty) = 0$ at $\delta > 0$ and $\delta < 0$, respectively. The finding that in the DMS case the HPL polarization tends to the theoretical limit in a high magnetic field means that the ground state of the impurity band is formed by a stress split state with angular momentum projection $F = \pm 1$ (the $F = 0$ state does not contribute to the magnetization). This assumption is supported by a recent study of the ferromagnetic resonance [22] which revealed that the cubic anisotropy fields are very large in (Ga,Mn)As (of the order of 2000 G). On the other hand, the splitting of the $F = 1$ Mn acceptor state can be induced by the strong electric field of ionized Mn acceptors. The fact that the high field limit of $\rho_c = 0.257$ is significantly lower than the expected value $\rho_c = 1$ [19] for an interband e-hh transition (recombination of spin unpolarized electrons with spin polarized heavy holes) supports our assignment of HPL to electron-impurity band transition. The polarization curves in paramagnetic ($B1$) as well as in ferromagnetic ($B3$) samples differ from that predicted by Eq. (1) [see solid line in Fig. 2(a) plotted for $B_{\text{eff}}(B) = B$ and $T = 5$ K]. For sample $B3$ [see Fig. 2(b)], one can distinguish two magnetic field regimes in the temperature range $T = 5$–60 K. First, we see a very fast HPL polarization increase at $B = 0$–0.5 T, and then the polarization slows down and tends to the theoretical limit at fields higher than $B = 10$ T. Such a behavior of polarization indicates that the ferromagnetic sample is microscopically not uniform and contains paramagnetic (slow polarization rate) as well as ferromagnetic (fast polarization rate) regions. The temperature increase destroys the ferromagnetic phase and thus increases the contribution of the paramagnetic phase to the HPL polarization. At temperatures above 90 K the magnetic field dependence of the polarization can be well approximated by Eq. (1) with $B_{\text{eff}}(B)$ [see solid line in Fig. 2(a)], which is the sum of the external field (B) and the exchange field induced by the Mn ions:

$$B_{\text{eff}}(B) = B + \frac{N_0\beta x S}{g_A\mu_B} B_{5/2}\left(\frac{g\mu_B SB}{kT}\right), \qquad (2)$$

where $g = 2$ is the g factor of the Mn ion, $N_0\beta$ is the $p - d$ exchange constant, x is the Mn concentration, and $B_{5/2}(B, T)$ is the Brillouin function. At low temperatures ($T \leq 50$ K) the polarization in a magnetic field tends to saturate much faster than one can expect for the effective field given by Eq. (1). Note, however, that even in the paramagnetic sample $B1$ the polarization [see Fig. 2(a)] shows a more complicated behavior than that expected for $B_{\text{eff}}(B)$ given by Eq. (2). This means that the Zeeman splitting of the impurity band at low temperature is enhanced by the ferromagnetic ordering of the Mn ions. The effective magnetic field acting on the impurity band in the ferromagnetic phase is much stronger than the external field and is proportional to sample magnetization $B_{\text{eff}}(B) = \lambda M(B, T)$, where λ is the Weiss constant and $M(B, T)$ is the sample magnetization. The magnetization of the sample in the direction of magnetic field (applied perpendicular to the sample layer) is proportional to the square of the spontaneous magnetization [$M(B, T) = M_s^2(T)B/2K$, where M_s is a spontaneous magnetization and K is an appropriate anisotropy coefficient] [23], whose easy axis in (Ga,Mn)As grown on GaAs substrate lies in the layer plane [1,6,10,22,24]. The temperature dependence of the spontaneous magnetization $M_s(T)$ and the Curie temperature of the ferromagnetic transition can be determined from the field dependence of the circular polarization presented in Fig. 2(b) for different temperatures. In the high temperature limit the series expansion of expression (1) [$\rho_c(B) \propto \frac{g\mu_B B_{\text{eff}}(B)}{kT}$] gives three different types of behavior of the polarization rate ($T[d\rho_c(B)/dB]_T$) on temperature (see Fig. 3). For single Mn acceptors (doping regime) the value $T[d\rho_c(B)/dB]_T = \text{const}$ does not depend on temperature in an external magnetic field (see dotted line in Fig. 3). In the paramagnetic phase of DMSs the impurity band polarization is given by the double Brillouin function [expressions (1) and (2)], therefore $T[d\rho_c(B)/dB]_T \propto 1/T$ (dashed lines in Fig. 3). In the ferromagnetic phase, $T[d\rho_c(B)/dB]_T \propto M_s(T)^2$. The solid lines in Fig. 3 represent the square of the spontaneous magnetization calculated in the frame of a simple mean-field model using the Brillouin function with $S = 5/2$. The solid and open circles in Fig. 3 show the dependence of $T[d\rho_c(B)/dB]_T$ on temperature for the ferromagnetic samples $B2$ and $B3$. The magnetization curves of both samples show clearly the transition from the ferromagnetic

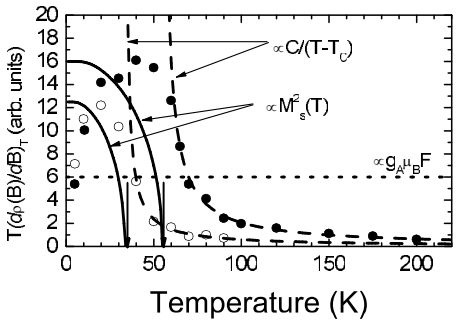

FIG. 3. Temperature dependence of $T[d\rho_c(B)/dB]_T$ for the two ferromagnetic samples $B2$ (open circles, $T_C = 35$ K) and $B3$ (solid circles, $T_C = 55$ K). The dashed lines represent the fit of $T(d\rho_c/dB)_T$ for samples $B2$ and $B3$ in the paramagnetic phase, while the solid lines show the expected behavior of $T(d\rho_c/dB)_T$ in the ferromagnetic phase using a simple mean-field approximation. The dotted line corresponds to single Mn acceptors.

to the paramagnetic phase at the Curie temperature marked by arrows in Fig. 3. Above the Curie temperature the value $T[d\rho_c(B)/dB]_T$ is proportional to the paramagnetic magnetization (M) of the sample and thus follows the Curie-Weiss law $T[d\rho_c(B)/dB]_T \propto M \propto C/(T - T_C)$ (dashed curves in Fig. 3). The Curie temperatures determined by the fit of the sample magnetizations in the paramagnetic phase are in good agreement with those measured by SQUID. Below the Curie temperature, one would expect a saturation of the spontaneous magnetization with decreasing temperature as illustrated by the solid curve obtained in a simple mean-field model. Contrary to expectation, the spontaneous magnetization shows an abrupt decrease at temperatures below $T \leq 10$ K. This polarization rate decrease can be related to the transition into an antiferromagnetic state of some neighboring Mn ions. Such antiferromagnetic ordering could lead to the decrease of the total magnetization of the sample, which, however, was not observed in our SQUID measurements. Therefore we conjecture that the polarization rate decrease at $T \leq 10$ K is induced by the $F = \pm 1$ state splitting. The cubic symmetry of the material indeed removes the twofold degeneracy of the ground $F = \pm 1$ impurity band state. This effect could manifest itself in the polarization as an effective temperature increase at $kT \leq \delta_4$ and $g_A\mu_B B \ll \delta_4$ (where δ_4 is the splitting of the $F = \pm 1$ state in two sublevels) [20]. Contrary to the holes localized in the impurity band, the monotonous saturation of spin polarization with temperature decrease was predicted for free holes in all range of temperatures below T_C.[14]

In conclusion, we demonstrated that even in heavily doped DMSs most of the valence band holes are either bound to Mn acceptors or confined in the impurity band. This finding rules out the indirect exchange interaction via degenerate holes (RKKY-like exchange) as a possible mechanism of the ferromagnetic phase transition in (Ga,Mn)As DMSs.

The ground $F = 1$ state of Mn acceptors in DMSs undergoes a strong splitting into unpolarized $F = 0$ and polarized $F = \pm 1$ states, the latter being the ground state of the impurity band. The cubic symmetry removes further the twofold degeneracy of the $F = \pm 1$ state. The temperature activated transition from the ground state $F = \pm 1$ into the unpolarized state ($F = 0$) can thus determine the Curie temperature in the model based on carrier mediated ferromagnetism in (Ga,Mn)As.

The ferromagnetic and paramagnetic phases are found to coexist in the whole temperature range below T_C in all DMS samples studied. This observation rather supports percolation based theories of ferromagnetism in (Ga,Mn)As DMSs.

One of us (V. F. S.) acknowledges the financial support from the Paul-Drude-Institute and Russian Foundation for Basic Research Grant No. 05-02-17782.

*Electronic address: sapega@dnm.ioffe.rssi.ru
Permanent address: Ioffe Physico-Technical Institute, Russian Academy of Sciences, 194021 St. Petersburg, Russia.
†Present address: Instituto de Ciencia de Materiales de Madrid, Cantoblanco, 28049 Madrid, Spain.

[1] H. Ohno *et al.*, Appl. Phys. Lett. **69**, 363 (1996).
[2] G. Prinz, Science **282**, 1660 (1998).
[3] S. A. Wolf *et al.*, Science **294**, 1488 (2001).
[4] H. Ohno *et al.*, Nature (London) **408**, 944 (2000).
[5] A. Oiwa *et al.*, Phys. Rev. Lett. **88**, 137202 (2002).
[6] H. X. Tang *et al.*, Phys. Rev. Lett. **90**, 107201 (2003).
[7] H. Akai, Phys. Rev. Lett. **81**, 3002 (1998).
[8] J. König *et al.*, Phys. Rev. Lett. **84**, 5628 (2000).
[9] J. Inoue *et al.*, Phys. Rev. Lett. **85**, 4610 (2000).
[10] T. Dietl *et al.*, Phys. Rev. B **63**, 195205 (2001).
[11] V. I. Litvinov and V. K. Dugaev, Phys. Rev. Lett. **86**, 5593 (2001).
[12] S. Sanvito *et al.*, Phys. Rev. B **63**, 165206 (2001).
[13] C. Timm, F. Schäfer, and F. von Oppen, Phys. Rev. Lett. **89**, 137201 (2002).
[14] S. Das Sarma *et al.*, Phys. Rev. B **67**, 155201 (2003).
[15] M. A. Alekseev *et al.*, Fiz. Tekh. Poluprovodn. **23**, 761 (1989) [Sov. Phys. Semicond. **23**, 479 (1989)].
[16] G. Fasol *et al.*, Phys. Rev. B **41**, 1461 (1990).
[17] I. Ya. Karlik *et al.*, Fiz. Tverd. Tela (Leningrad) **24**, 3550 (1982) [Sov. Phys. Solid State **24**, 2022 (1982)].
[18] W. Schairer and M. Schmidt, Phys. Rev. B **10**, 2501 (1974).
[19] *Optical Orientation*, edited by F. Meyer and B. P. Zakharchenya (North-Holland, Amsterdam, 1984).
[20] N. S. Averkiev *et al.*, Fiz. Tverd. Tela (Leningrad) **30**, 765 (1988) [Sov. Phys. Solid State **30**, 438 (1988)].
[21] V. F. Sapega *et al.*, Phys. Status Solidi (b) **226**, 339 (2001).
[22] X. Liu *et al.*, Phys. Rev. B **67**, 205204 (2003).
[23] S. Chikazumi, *Physics of Ferromagnetism* (Clarendon Press, Berlin, 1998).
[24] G. P. Moore *et al.*, J. Appl. Phys. **94**, 4530 (2003).